

## Research Article

# Effect of Temperature on the Viscoelastic Properties of Carbon Nanotube Reinforced Polypropylene Composites

Jun Huang <sup>1</sup>, Denis Rodrigue,<sup>2</sup> and Ling Dong <sup>3</sup>

<sup>1</sup>College of Civil Engineering and Architecture, Wenzhou University, Wenzhou 325035, China

<sup>2</sup>Department of Chemical Engineering, Laval University, Quebec City G1V 0A6, Canada

<sup>3</sup>School of Arts and Culture Communication, Guangxi University of Science and Technology, Liuzhou 545006, China

Correspondence should be addressed to Ling Dong; 100001058@gxust.edu.cn

Received 3 January 2021; Revised 5 April 2021; Accepted 12 April 2021; Published 24 April 2021

Academic Editor: Matjaz Valant

Copyright © 2021 Jun Huang et al. This is an open access article distributed under the Creative Commons Attribution License, which permits unrestricted use, distribution, and reproduction in any medium, provided the original work is properly cited.

Finite element method (FEM) is used to analyze the mechanical properties of carbon nanotubes (CNTs) reinforced polypropylene (PP) composites. Firstly, polypropylene is assumed as a viscoelastic material, while carbon nanotubes are assumed as linear elastic materials to study the effect of temperature on the mechanical properties of neat PP and CNT/PP nanocomposites. Secondly, to compare the viscoelastic properties of neat PP and CNT/PP nanocomposites, the relaxation time at a specific temperature is used to investigate the relaxation of the nanocomposites for fixed tensile displacements. Thirdly, the effect of CNT volume fraction on the viscoelastic properties of nanocomposites is studied at different temperatures. Finally, to better understand the stress distribution along the CNT axial direction, a single carbon nanotube is isolated in the matrix to compare the stress distribution with nonisolated CNTs.

## 1. Introduction

Polypropylene (PP) is used in a wide variety of applications including packaging, textiles, and automotive components. Today, several interesting results have been reported for different PP structures: branching of linear Ziegler–Natta polypropylene [1], viscoelastic flow analysis, and surface morphology of injection-molded PP [2], viscous properties [3], etc. Peng et al. [4] proposed a novel phenomenological model consisting of springs, dashpot, stress-locks, and sliders to describe the nonlinear viscoelastic properties of PP via indentation creep tests at different load levels. However, PP has a very narrow thermoforming window and the mechanical properties rapidly decrease with increasing temperature [5]. Drozdov reported some observations on PP in uniaxial tensile tests with various strain rates and relaxation tests at temperatures ranging from 23 to 120°C [6]. For this range of temperature, the stress ( $\sigma$ ) monotonically increased with strain rate while monotonically decreased with temperature. Furthermore, Lesan-Khosh et al. [7] measured the local and global mechanical properties at

various temperatures and strain rates, while reporting some relations between both types of mechanical properties.

As a low density material, PP is widely used in toys, package, decoration, etc. However, PP has lower elastic modulus and strength and poor impact resistance; to improve the mechanical properties of polymers, different types of particles with specific properties are often added into the matrix. Nano-clay with different content was blended with PP to increase the thermal and viscoelastic properties [8]. Peng et al. [9] proposed a phenomenological thermo-mechanical viscoelastic constitutive model for PP-wood composites, while Karaduman et al. [10] investigated the viscoelastic properties of jute/PP nonwoven reinforced composites.

Although fillers can improve the viscoelastic properties of PP, nanoparticles are more interesting to modify the viscosity of PP due to their higher specific surface area [11]. In particular, carbon nanotubes (CNTs) have been extensively studied due to their unique combination of mechanical, thermal, and chemical properties [12–14]. For this reason, they have high potential to modify polymer matrices

[15–19]. Because of their high stiffness and high strength, single-wall CNTs (SWCNT) can lead to substantial increases in mechanical properties even at very low content (less than 1 wt.%) [20]. Arshid et al. [21] presented that CNTs' volume fraction elevation caused mechanical properties improvement. However, with increasing CNT content, it is not easy to disperse them inside highly viscous matrices like PP melts. Nevertheless, Deng et al. [22] showed that efficient reinforcement can be obtained at only 0.5 wt.% CNT. To further analyze this condition, a computational method was presented to account for the effect of MWCNT agglomeration on the mechanical properties of the nanocomposites, and the predicted modulus was in good agreement with the experiment data [23]. In addition, the effect of CNT curvature is also not ignored on mechanical properties of composites. The results obtained from [24] indicated that the reinforcing capacity of CNTs reduces drastically even with a small waviness as compared to the straight CNTs. In fact, the most important factor affecting the improvement level was the PP-CNT interfacial layer [25]. In particular, the formation of a trans-crystalline layer around the CNT can improve the stress transfer from the amorphous continuous phase (PP) to the rigid dispersed phase (CNT). Furthermore, CNT addition can improve Young's modulus and yield strength of nanocomposites under low and high velocity impact [26]. Li et al. [27] investigated the effects of multiwall carbon nanotubes on the mechanical properties of isotactic polypropylene composites under pressure. The results showed that multiwall carbon nanotubes can efficiently increase Young's modulus, yield strength, and elongation when the composites break and when the pressurization rate is lower than 5.0 MPa/s. CNTs can also be used with other reinforcements (such as glass fiber) to produce hybrid systems improving the modulus and tensile strength of composites further [28]. Finally, there is possibility to surface modify the CNT to improve the interfacial stress transfer leading to improved mechanical properties of polypropylene composites. More details can be found in a review by Bikiaris [29].

Similar to mechanical improvement, CNT addition has a direct effect on the rheological properties of nanocomposites. The addition of CNTs can increase the polypropylene viscosity leading to a shift from a fluid-like to a solid-like behavior [30]. This is especially the case when the fraction is above 2 wt.% (critical percolation threshold). A similar work was presented by Jia et al. [31] where CNT addition was shown to decrease the recovered strain at higher temperatures. For example, the unrecovered strain decreased by 53% and 73% at 1.0% and 2.8 vol.% CNT, respectively. Furthermore, Shim et al. [32] investigated the storage/loss modulus and shear viscosity of nanocomposites with increasing CNT content. Via dynamic frequency sweeps, the complex viscosity and  $\tan \delta$  (ratio of loss modulus to storage modulus) behavior were studied by Wang et al. [33]. On the contrary, the finite element method (FEM) was extensively used in engineering as a powerful numerical analysis tool [34]. Montazeri and Naghdabadi [35] investigated the buckling of CNT reinforced polyethylene composites when the matrix was assumed to be a

viscoelastic material. Duncan et al. [36] analyzed the effect of CNT aspect ratio and epoxide-terminated surface modification on the glass transition temperature ( $T_g$ ) and loss modulus ( $E''$ ) of nanocomposites. Swain and Roy [37] showed that quick vibration mitigation was possible by adding carbon nanotubes into the 934 epoxy according to micromechanics principles. Hirane et al. [38] further investigated the static and free vibration of sandwich plates with layerwise finite element method, and the results showed that the developed model is promising in the accuracy and fast rate of convergence.

In our previous works [39, 40], single-wall carbon nanotubes were randomly distributed into PP and numerically studied via finite element analysis. SWCNT was shown to efficiently improve the mechanical properties of nanocomposites at room temperature under different loading conditions (uniaxial or multiaxial). In this work, literature data from [7] are used to validate our model at low deformation (elastic deformation). Then, FEM simulations are performed to investigate the viscoelastic properties of SWCNT reinforced PP nanocomposites over a range of temperatures (20, 40, 60, and 80°C) to determine the performance of these materials above room temperature which is important for engineering applications like automotive and packaging which are subjected to different temperature and long-term deformation. As a starting simplification, it is assumed that the viscous behavior of PP at 20°C is negligible.

## 2. Numerical Models

A representative volume element (RVE) is used to evaluate the viscoelastic properties of PP-based composites. To study the mechanical behavior of this RVE via the finite element method, the effect of SWCNT content on the stress-time curves of SWCNT/PP nanocomposites under different temperatures is investigated. The numerical specimen is assumed to be a cylinder for which the length and end diameter are constant at 600 nm and 200 nm, respectively. SWCNT is randomly distributed in the cylinder (PP matrix) along the deformation direction. The SWCNT diameter is taken as 1.4 nm, and the length is 400 nm [40]. As a first step, the SWCNT volume fraction is fixed at 0.5%. Then, the SWCNT content was increased from 0.5% to 1.5%. All specimens are created in MATLAB and tested for uniaxial tension. Figure 1(a) shows the mechanical model of the nanocomposites. The node displacements of the bottom along the  $x$ ,  $y$ , and  $z$  directions are constrained. A displacement taken as 0.1 nm for tensile numerical simulations is applied to the nodes of the top surface of the nanocomposites. The reaction forces are calculated on the surface where the displacement conditions are given.

The commercial finite software MSC.MARC is used because of its wide range of element libraries [41]. Two types of finite elements are selected here: Element 7 and Element 98. Element 7 is an eight-node, isoparametric, arbitrary hexahedron with trilinear interpolation functions, and the strains tend to be constant throughout the element. This results in a poor representation of the shear behavior. The stiffness of this element is formed using eight-point

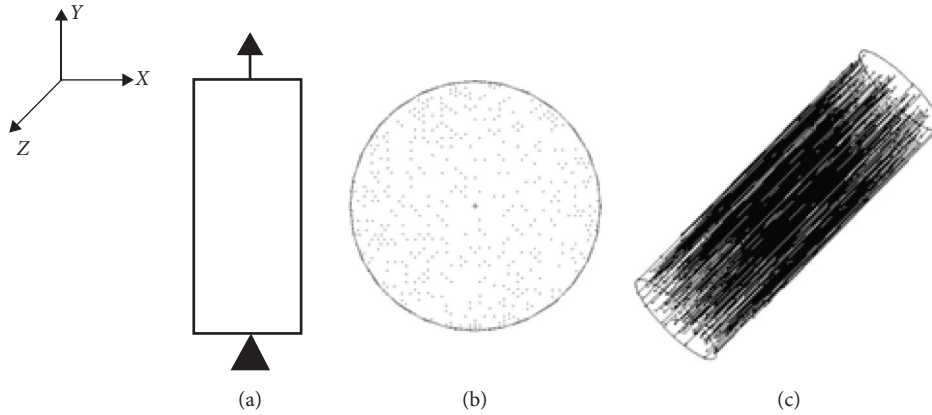


FIGURE 1: Numerical model for (a) mechanical model; (b) top view of the model; (c) side view of SWCNT/PP.

Gaussian integration. For a nearly incompressible behavior, including plasticity or creep, it is advantageous to use an alternative integration procedure. This element can be used for all constitutive relations. Here, Element 7 is used to simulate the matrix (PP). No significant differences between the results obtained from 3-D truss or beam elements were found based on preliminary trials. Hence, the beam element was selected to simulate the SWCNT. Element 98 is a thick straight beam including transverse shear effects with not only linear elastic material response, but also nonlinear elastic and inelastic material response. This element uses a one-point integration scheme located at the midspan leading to an exact calculation for bending and a reduced integration scheme for shear. Element 98 has two nodes, and each node has six degrees of freedom including three translations and three rotations. In addition, linear interpolation is used for the axial and transverse displacements, as well as for rotation. Element 98 is used to model the reinforcement (SWCNT). Each SWCNT fiber length is 400 nm, and the corresponding element length is 10 nm.

### 3. Mechanical Properties

MSC.MARC has two models to represent viscoelastic materials. The first is a Kelvin–Voigt model, while the second is a general hereditary integral approach. The Kelvin–Voigt model allows the rate of change of the inelastic strain to be a function of the total stress and the previous strain. The Kelvin–Voigt behavior (viscoelasticity) is modeled by assuming an additional creep strain. As represented in the Kelvin–Voigt model, the stress-strain relationships depend on the current stress and strain state. However, the complete stress history is necessary. In terms of the hereditary integrals or Duhamel integrals, the constitutive behavior is most readily expressed as these integrals are formed by considering the stress or strain build-up at successive times. Two equivalent integral forms exist: the stress relaxation form and the creep function form. Here, the stress relaxation form is used.

In the stress relaxation form, the deviatoric and volumetric behavior of an isotropic viscoelastic material are

assumed to be fully decoupled and described by a time-dependent shear and bulk moduli. The bulk modulus is generally assumed to be time independent. However, this is an unnecessary restriction of the general theory. In this work, the bulk modulus is neglected, and the shear modulus can be expressed in a Prony series as given in [42]:

$$G(t) = G^\infty + \sum_{i=1}^n G^i e^{-(t/\tau_i)}, \quad (1)$$

$$G^0 = G^\infty + \sum_{i=1}^n G^i, \quad (2)$$

where  $G(t)$  is the shear-stress relaxation functions, they represent the response to a unit applied strain and have characteristic relaxation times associated with them,  $G^\infty$  represents the long-term shear modulus, and  $\tau_i$  is a positive time constant (relaxation time). For short time ( $t=0$ ), equation (1) can be written as equation (2). It describes the instantaneous elastic effect. In our case, the value of  $n$  was taken as one to compare the effect of relaxation time on viscoelastic properties of composites.

Here, PP is assumed to be a viscoelastic material for the temperature range studied (20 to 80°C). When the temperature is 20°C, the relaxation modulus  $G^n$  is considered negligible, while the values for higher temperatures are taken from [7]. SWCNT is assumed to be globally isotropic and characterized by a linear elastic behavior. In this case, the following elastic constants are selected: Young's modulus ( $E = 1030$  GPa) and Poisson's ratio ( $\nu = 0.063$ ) [39].

Finally, the SWCNT/PP nanocomposite is approximated as a two-phase material, and the SWCNT-PP interface is assumed to have perfect adhesion (no slip here, which will be studied in a future work). The mechanical properties of each component are listed in Table 1. All the numerical simulations are convergent.

### 4. Results

To characterize the viscoelastic behavior of the materials, the relaxation modulus is used to depict the time dependence of

TABLE 1: Mechanical properties of the components.

Mechanical properties	SWCNT	Polypropylene
Young's modulus (GPa)	1030	1.88
Tensile strength (GPa)	30	0.0348
Poisson ratio	0.063	0.40

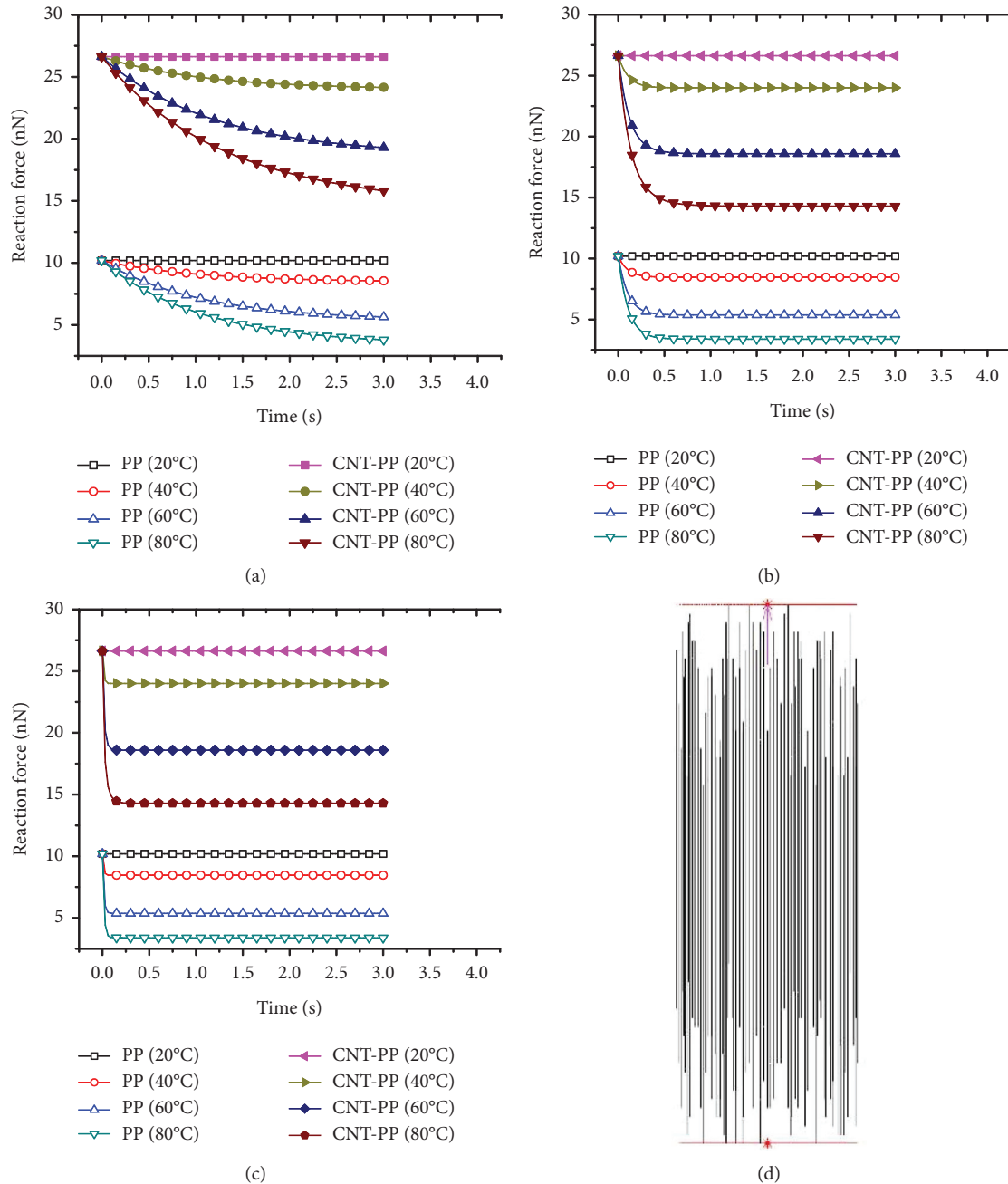


FIGURE 2: Tensile reaction force-time curves of the numerical specimens for different temperature: (a) relaxation time  $t = 1$  s; (b) relaxation time  $t = 0.1$  s; (c) relaxation time  $t = 0.01$  s; (d) SWCNT in the matrix.

SWCNT/PP nanocomposites and neat PP. On the contrary, SWCNT content will play an important role on the mechanical properties of the nanocomposites. In these

numerical simulations, the effect of SWCNT volume fraction on the viscoelasticity of the nanocomposites and neat PP is investigated.

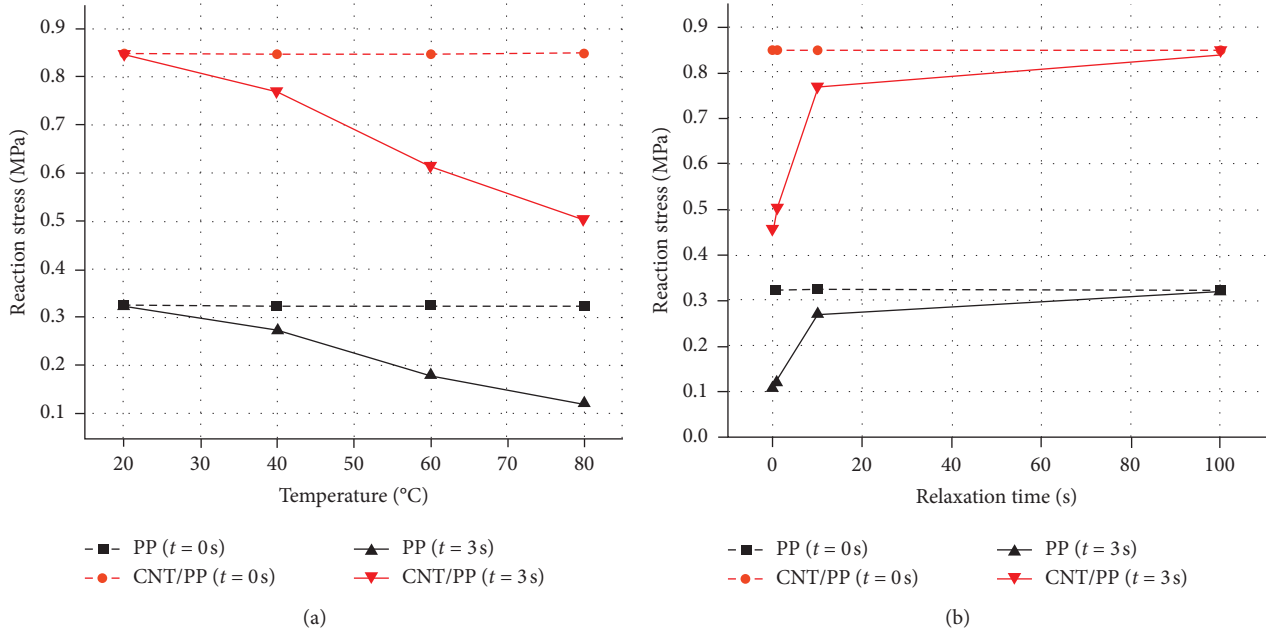


FIGURE 3: Effects of temperature and relaxation time on viscoelastic properties of PP and CNT/PP with CNT volume fraction of 0.5%. (a) Temperature; (b) relaxation time.

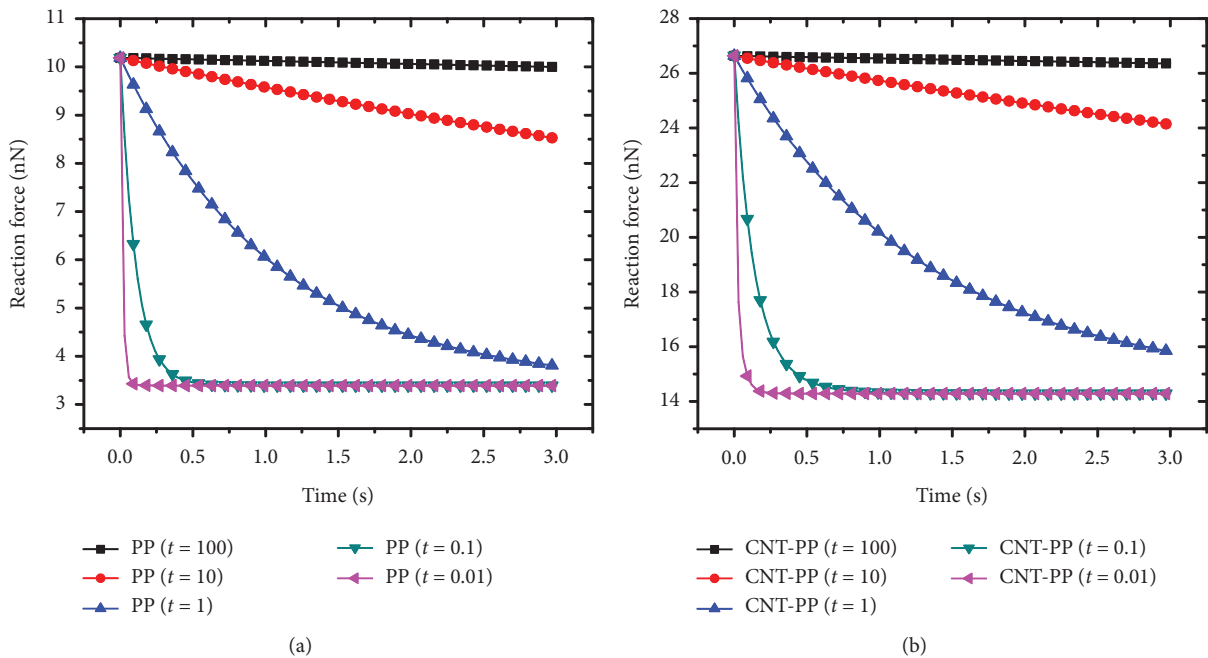


FIGURE 4: Reaction force-time curves with different relaxation time: (a) neat polypropylene; (b) SWCNT/PP nanocomposites.

**4.1. Effect of Temperature.** In this work, the global mechanical properties of PP are selected [7]. The elastic modulus of PP is taken as 1880 MPa, which is the value at 20°C. When the temperature increases to 40, 60, and 80°C, the elastic modulus is taken as 1536 MPa, 946 MPa, and 586 MPa, respectively. To investigate the viscoelastic properties of PP and SWCNT/PP composites, the loss modulus can be transformed to the time-dependent relaxation modulus which is 122.8 MPa, 333.5 MPa,

or 462.1 MPa in terms of the relationship between the elastic modulus and the shear modulus. Here, the variation of the relaxation time is used to simulate the viscoelastic properties of the neat PP and SWCNT/PP nanocomposites at various temperatures. The numerical results are plotted in Figure 2. In all cases, the loading displacement is fixed at 0.1 nm, and the SWCNT volume fraction is fixed at 0.5%, so the reaction forces, which are the response to the displacement, are obtained.

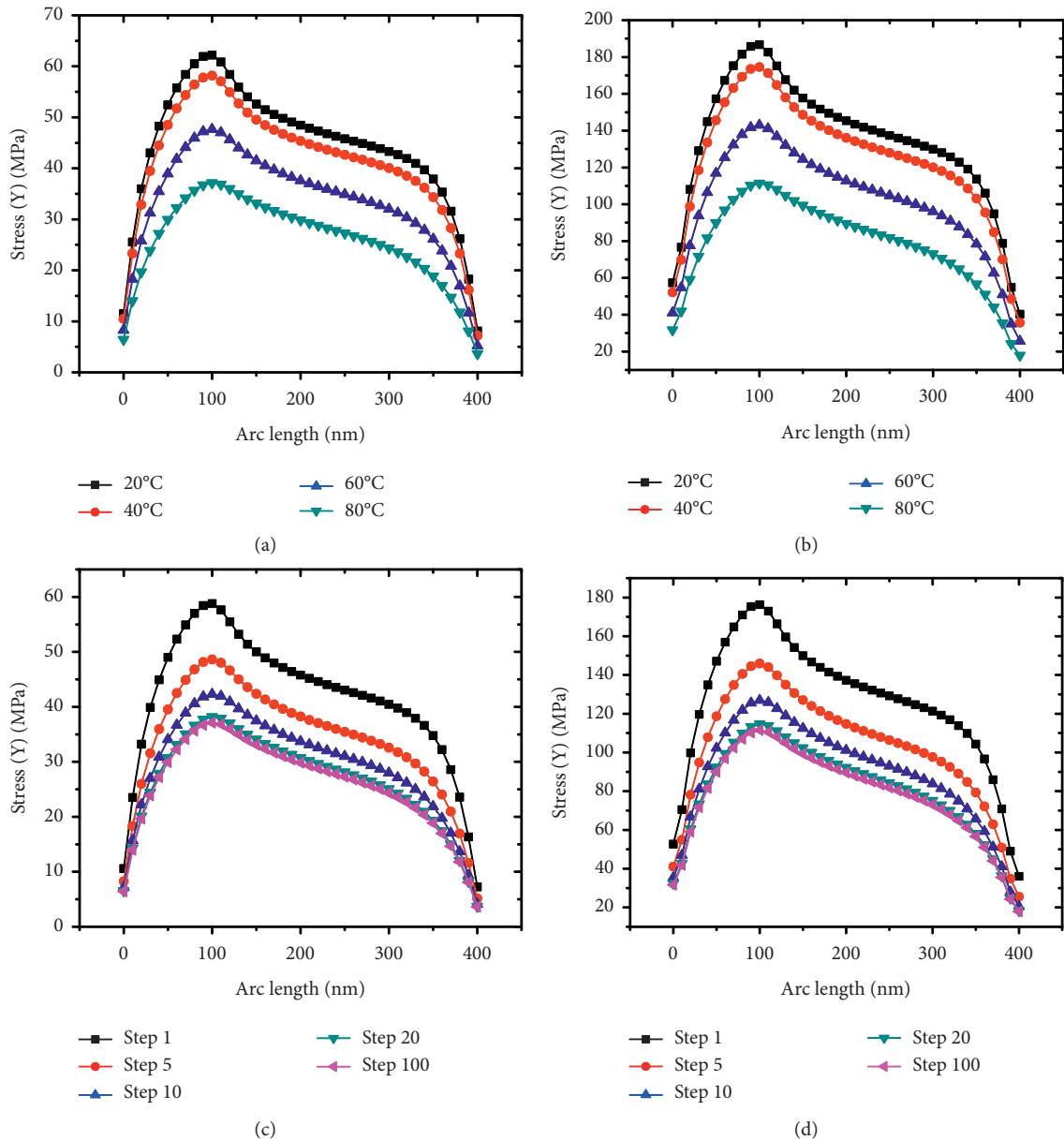


FIGURE 5: Results for one SWCNT in a nanocomposite for a relaxation time of  $t = 0.1$  s, (a) stress-arc length curves for nonisolated SWCNT; (b) stress-arc length curves for isolated SWCNT; (c) stress-arc length curves at different loading steps for nonisolated SWCNT; (d) stress-arc length curves at different loading steps for isolated SWCNT.

Figure 2(a) shows the reaction force-loading time curves of PP and SWCNT/PP composites at a fixed relaxation time of 1 s. From this plot, it is clear that for all cases (neat PP and SWCNT/PP), the reaction forces decrease (relaxation phenomenon) with time. It is also easy to see that increasing the temperature decreases the viscoelastic properties of the matrix and nanocomposites. For example, at  $T = 80^\circ\text{C}$  and  $t = 3$  s, the reaction force for neat PP decreases from 10.188 nN to 3.799 nN at  $20^\circ\text{C}$  (63%). However, for the nanocomposites, the reaction force decreases only from 26.636 to 15.821 nN (41%), indicating a better resistance of the nanocomposite at higher temperature compared to the neat matrix. The plot also shows that to get the same deformation, higher loading must be applied on the nanocomposites compared to the neat matrix. For example,

when the temperature is  $60^\circ\text{C}$  and  $t = 3$  s, the reaction force of SWCNT/PP is 19.294 nN, which is higher (2.42 times) than 5.641 nN for the neat PP. Similar trends for a relaxation time of 0.1 or 0.01 s are reported in Figures 2(b) and 2(c), respectively. Compared with Figure 2(a), the relaxation time has a direct effect on the viscoelastic properties of PP and SWCNT/PP nanocomposites. In all cases, increasing the relaxation time decreases the reaction force.

To clearly compare the effects of the temperature and relaxation time on the viscoelastic properties of composites, the specific loading time (0 s and 3 s) and CNT content (0.5%) are selected to analyze the results. Considering the cross-sectional area of the specimen, the reaction forces can be transferred to be the reaction stresses. The related data are



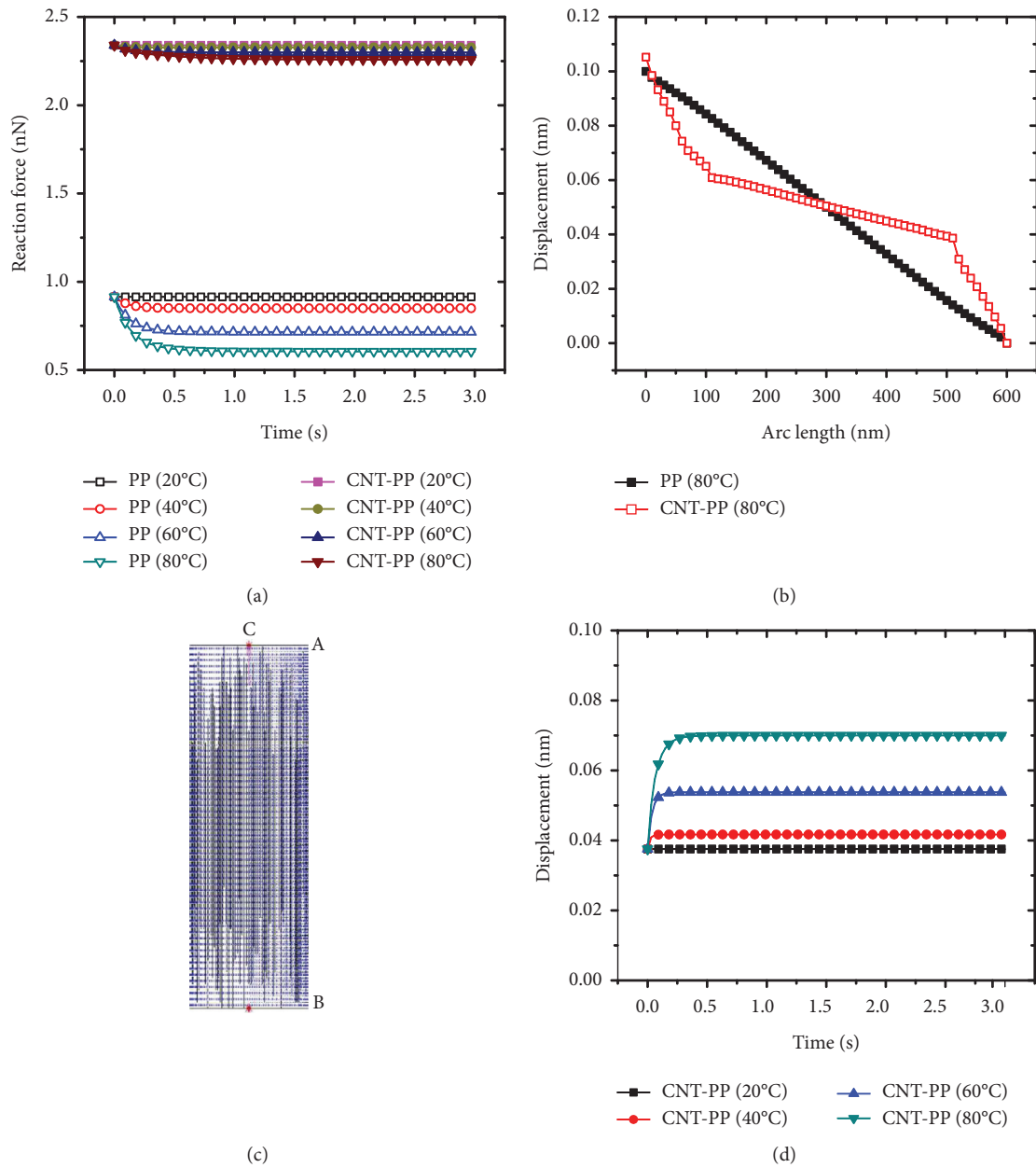


FIGURE 6: (a) Reaction force-time curves of PP and SWCNT/PP nanocomposites at node A for different temperature; (b) the displacement-arc length curves of the nodes along path AB at 80°C; (c) the position of nodes A and B; (d) the displacement-time curves of node C for SWCNT/PP nanocomposites when the load is fixed at 10 nN.

plotted in Figure 3(a). It can be seen that the reaction stresses of CNT/PP is much larger than that of PP whatever the loading time is taken as 0 s or 3 s. When the loading time is 3 s, the reaction stresses decrease with the increasing temperature.

Figure 4 presents the effect of the relaxation time on the viscoelastic properties of the neat PP and SWCNT/PP nanocomposites at 80 C. From Figure 4(a), the reaction force for neat PP decreases very rapidly with decreasing relaxation time. For example, at 3 s, when the relaxation time is 100, 10, 1, 0.1, and 0.01 s, the reaction force decreases from 9.999 nN to 8.515, 3.799, 3.393, and 3.393 nN, respectively. The same trend occurs in Figure 4(b). However, because of the SWCNT reinforcement, the reaction force is much higher

and decreases more slowly than for neat PP. At 3 s, with the relaxation time taken as 100, 10, 1, 0.1, and 0.01 s, the reaction force for SWCNT/PP nanocomposites decreases from 26.356 nN to 24.128, 15.821, 14.289, and 14.289 nN, respectively. At the specific loading time and CNT content (0.5%), the effects of the relaxation time on the viscoelastic properties of composites are plotted in Figure 3(b). It is clear that the reaction stresses of composites increase with the relaxation time increasing. If the relaxation time is larger enough, the viscoelastic property of composite is more close to the elastic property.

To better determine the effect of SWCNT on the mechanical properties of the neat polypropylene and

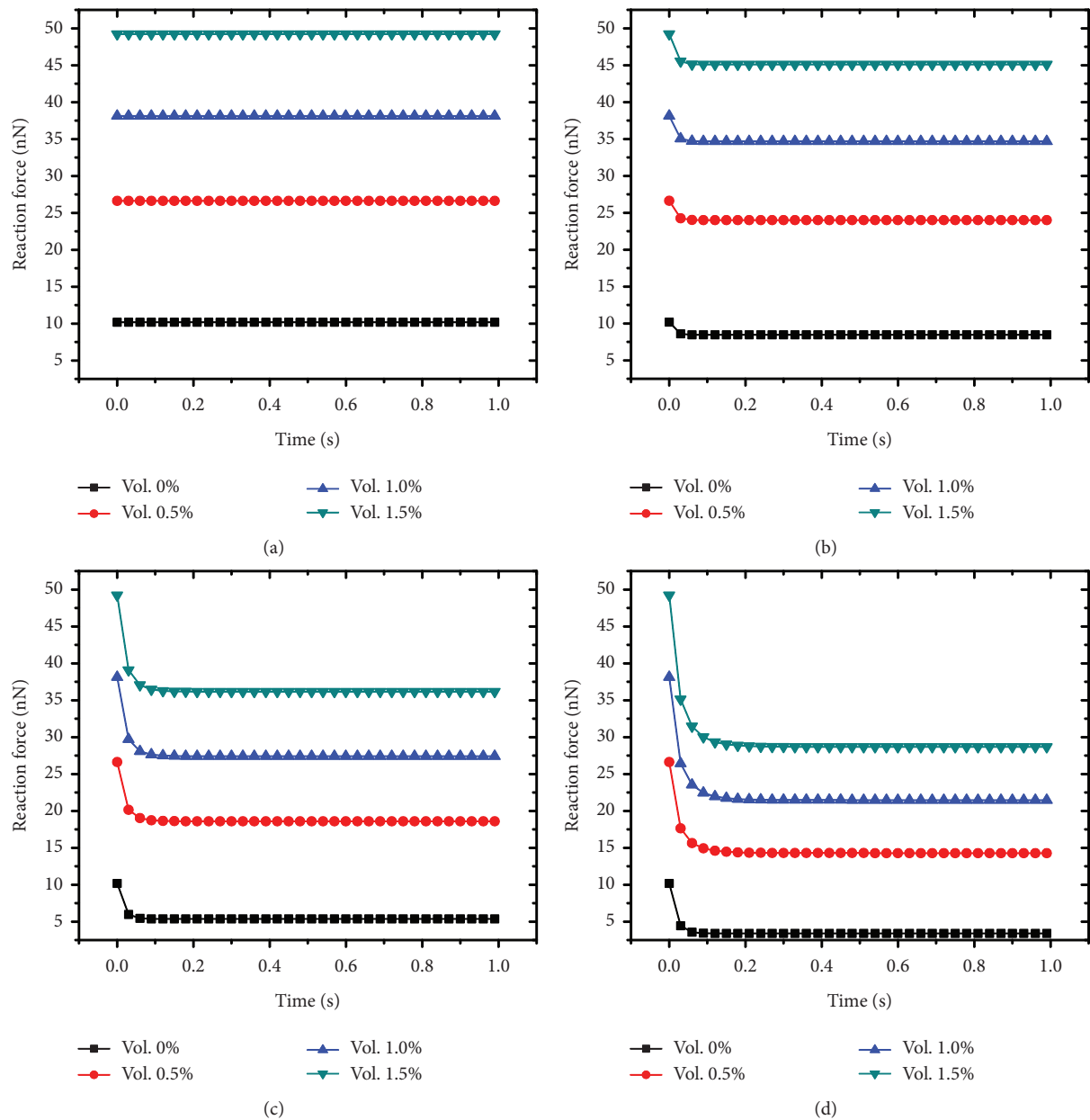


FIGURE 7: Reaction force-time curves of the nanocomposites with different SWCNT content for a 0.1 nm loading displacement at different temperatures: (a) 20; (b) 40; (c) 60; (d) 80°C.

nanocomposites at different temperature, the analyzed results of a single fiber (SWCNT) are isolated from the composite, so the stresses, strains, and other mechanical properties of the SWCNT can be separately determined. Figures 5(a) and 5(b) show the stress distributions at different nodes for one SWCNT nonisolated and isolated element. Nonisolated element includes the matrix element and carbon nanotube element, which can undertake the stress and deformation together, while the isolated element only includes the carbon nanotube element to withstand the stress and deformation. For the nonisolated elements, when the arc length is 100 nm, the stresses reach a maximum value of 62.213, 58.167, 47.649, and 37.129 MPa as the temperature increases from 20 to 40, 60, and 80°C, respectively. For the

isolated elements, the maximum stresses are from 186.703 to 174.568, 143.025, and 111.473 MPa for the same temperatures. From these results, it can be seen that SWCNT can sustain more stresses and restrict more effectively the deformation of the polypropylene matrix, especially as the temperature increases.

To better understand the stress distributions on the nodes, the stresses at different loading steps are presented in Figures 5(c) and 5(d) at a temperature of 80°C. From these results, it is clear that the stresses initially relax very quickly, but after step 20, the decreasing trend is slower.

Figure 6(a) shows the reaction force-time curves of the neat PP and SWCNT/PP nanocomposites at node A (Figure 6(c)). With increasing temperature, the trends are



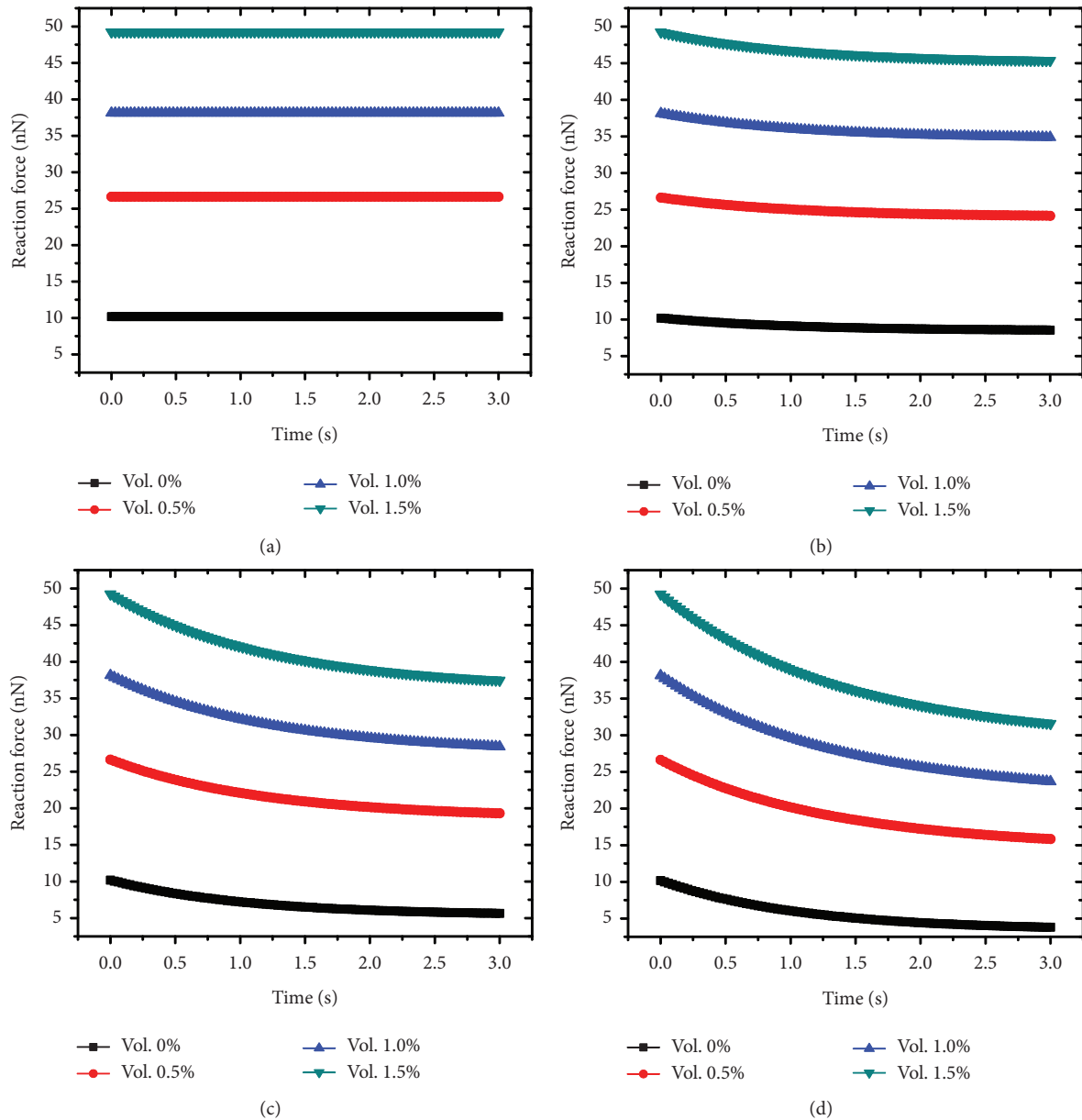


FIGURE 8: Reaction force-time curves of the nanocomposites with different SWCNT content for a 0.1 nm loading displacement: (a) 20; (b) 40; (c) 60; (d) 80°C.

similar to Figure 2. To keep the same deformation, the node A will be set at higher loading. In general, because node B is fixed, it has no displacement, so node A is given a constant displacement of 0.1 nm. For the neat PP, the nodes between A and B will follow a linear displacement. However, for SWCNT/PP nanocomposites, the distribution of SWCNT in the matrix will affect the displacement between nodes A and B as reported in Figure 6(b). The displacements close to nodes A and B change very rapidly at 80°C; for this case, there is a nonlinear deformation along the axial direction for SWCNT/PP nanocomposites.

For a viscoelastic material, the deformation will increase if the load is constant. To analyze the viscoelastic properties for this case, a load of 10 nN is applied to the top of SWCNT/PP nanocomposites. The numerical results for the

temperature selected are plotted in Figure 6(d). It can be seen that the initial deformations of the nanocomposites are larger. However, after 0.3 s, the displacements of the nanocomposites are negligible. As expected, the creep of SWCNT/PP nanocomposites increases with temperature; i.e., higher deformation over a longer period of time.

4.2. *Effect of SWCNT Content.* Assuming a relaxation time of 0.01 s, three SWCNT volume fractions (0.5, 1.0, and 1.5%) are selected to simulate the viscoelastic properties of SWCNT/PP nanocomposites and compare them with the viscoelasticity of the neat polypropylene. The numerical results for 20, 40, 60, and 80°C are plotted in Figures 7(a) to 7(d) assuming there is negligible relaxation for SWCNT/PP

and neat PP at 20°C. In Figure 7(a), the relaxation modulus of the neat PP and SWCNT/PP are negligible, while the presence of SWCNT only improves the matrix rigidity. When the SWCNT content is 0.5, 1.0, and 1.5%, the reaction forces increase to 26.636, 38.119, and 49.230 nN, respectively, compared to 10.188 nN for the neat PP. In Figure 7(b), the relaxation modulus at 40°C of PP is 122.8 MPa and relaxation occurs. When the time is 0.03 s, the reaction force of SWCNT/PP nanocomposites dropped to 24.251, 35.034, and 45.529 nN compared to 8.594 nN for the neat PP, and then the reaction forces do not change. When the temperature reaches 60°C and 80°C, the relaxation modulus of PP is 333.5 MPa and 462.1 MPa, respectively. In these two cases, the relaxation phenomena are more obvious, especially at 80°C; i.e., the relaxation modulus of PP is 462.1 MPa, and the reaction force of SWCNT/PP dropped from 49.230 nN to 28.675 nN with 1.5% of SWCNT. In general, with increasing temperature, the relaxation phenomena of the composites are more obvious with increasing temperature; i.e., higher variation levels over longer periods of time.

To compare the effects of the relaxation time on the viscoelastic properties of SWCNT/PP nanocomposites with different SWCNT content, a relaxation time of 1 s is assumed. The results for 20, 40, 60, and 80°C are plotted in Figures 8(a) to 8(d). Similarly, in Figure 8(a), the relaxation moduli of neat PP and SWCNT/PP are negligible, while SWCNT only improves the matrix rigidity. With increasing temperature, the reaction force of the composites along the loading direction decreases more rapidly. Especially at 80°C, the reaction force of SWCNT/PP in Figure 8(d) dropped from 49.230 nN to 39.054 nN (time = 1 s) and 31.570 nN (time = 3 s) with 1.5% of SWCNT. Compared with Figure 8(d), when the relaxation time changes from 0.01 s to 1 s, whatever the SWCNT volume fraction, the viscous properties of the composites are not obvious. That is to say, from the simulations (compare Figure 7 with Figure 8), the viscoelastic properties of the composites are more affected by temperature and relaxation time than the SWCNT content for the range of conditions investigated.

## 5. Conclusions

In this work, the relaxation time and relaxation modulus were used to depict the viscoelastic properties of polypropylene (PP) as a matrix. Then, the effects of temperature (20–80°C) and single-wall carbon nanotube (SWCNT) content (0.5–1.5 vol.%) were investigated using numerical simulations (finite element method) to determine the viscoelastic properties of PP and SWCNT/PP nanocomposites for uniaxial tension loading. From the results obtained, the main conclusions are as follows:

- (1) Keeping the loading displacement constant, the reaction forces decreased with time (relaxation). As expected, the changes were faster with increasing temperature and decreasing relaxation time. When the loading time is fixed 0 s and 3 s, the SWCNT volume fraction is fixed 0.5%, it is clear that the stress capacity of PP or CNT/PP decreases with increasing

temperature, especially the temperature is taken as 80°C. Similarly, if the relaxation time is greater enough, the fluid-like characteristic of composite is more close to the solid-like characteristic.

- (2) Whatever the temperature and relaxation time, SWCNT can very efficiently improve the mechanical properties of the nanocomposites (rigidity) when the loading displacement is fixed, even at low content. However, increasing SWCNT volume fraction led to higher stiffness and strength of the SWCNT/PP nanocomposites. On the contrary, when the loading force was fixed, SWCNT efficiently restricted the deformation of the nanocomposites. As SWCNT content increased, the creeping behavior of the nanocomposites became less important.
- (3) By isolating a SWCNT in the matrix, it was possible to show that SWCNT can undertake more stresses than the neat PP in SWCNT/PP nanocomposites. At the same time, comparing the homogeneous material, SWCNT is randomly distributed in the matrix, so the stresses distribution in the matrix changes for different SWCNT locations. The nodes rigidly connected to SWCNT undertook more stresses than those of the neat PP regions.

## Data Availability

All data, models, and code generated or used during the study appear in the published article.

## Conflicts of Interest

The authors declare that they have no conflicts of interest.

## Acknowledgments

This study was supported by the Zhejiang Provincial Natural Science Foundation of China (Grant number: LY18E080028) and funded by the National Natural Science Foundation of China (Grant number: 51568009) and the Wenzhou Science and Technology Project, China (Grant number: S20190001).

## References

- [1] C. He, S. Costeux, P. Wood-Adams, and J. M. Dealy, "Molecular structure of high melt strength polypropylene and its application to polymer design," *Polymer*, vol. 44, no. 23, pp. 7181–7188, 2003.
- [2] Y. Kobayashi, Y. Otsuki, and T. Kanai, "Viscoelastic flow analysis of surface morphology on injection-molded polypropylene," *Polymer Engineering & Science*, vol. 50, no. 11, pp. 2182–2189, 2010.
- [3] D. Tscharnuter, M. Jerabek, Z. Major, and G. Pinter, "Uniaxial nonlinear viscoelastic viscoplastic modeling of polypropylene," *Mechanics of Time-dependent Materials*, vol. 16, no. 3, pp. 275–286, 2012.
- [4] G. Peng, Y. Ma, Y. Feng, Y. Huan, C. Qin, and T. Zhang, "Nanoindentation creep of nonlinear viscoelastic polypropylene," *Polymer Testing*, vol. 43, pp. 38–43, 2015.

- [5] C. P. J. O'Connor, P. J. Martin, and G. Menary, "Viscoelastic material models of polypropylene for thermoforming applications," *International Journal of Material Forming*, vol. 3, pp. 599–602, 2010.
- [6] A. D. Drodzov, "Effect of temperature on the viscoelastic and viscoplastic behavior of polypropylene," *Mechanics of Time-dependent Materials*, vol. 14, no. 4, pp. 411–434, 2010.
- [7] R. Lesan-Khosh, R. Bagheri, and S. Asgari, "Nanoindentation of isotactic polypropylene: correlations between hardness, yield stress, and modulus on the local and global scales," *Journal of Applied Polymer Science*, vol. 121, no. 2, pp. 930–938, 2011.
- [8] M. A.-h. Ali and R. H. Elleithy, "Viscoelastic properties of polypropylene/organo-clay nano-composites prepared using miniature lab mixing extruder from masterbatch," *Journal of Applied Polymer Science*, vol. 121, no. 1, pp. 27–36, 2011.
- [9] X. Q. Peng, H. L. Yin, J. Chen, and X. Liu, "A phenomenological thermal-mechanical viscoelastic constitutive modeling for polypropylene wood composites," *Advances in Materials Science and Engineering*, vol. 2012, Article ID 793617, 7 pages, 2012.
- [10] Y. Karaduman, M. M. A. Sayeed, L. Onal, and A. Rawal, "Viscoelastic properties of surface modified jute fiber/polypropylene nonwoven composites," *Composites Part B: Engineering*, vol. 67, pp. 111–118, 2014.
- [11] J. T. Kalathi, G. S. Grest, and S. K. Kumar, "Universal viscosity behavior of polymer nanocomposites," *Physical Review Letters*, vol. 109, no. 19, 2012.
- [12] V. C. Tung, L.-M. Chen, M. J. Allen et al., "Low-temperature solution processing of Graphene–Carbon nanotube hybrid materials for high-performance transparent conductors," *Nano Letters*, vol. 9, no. 5, pp. 1949–1955, 2009.
- [13] W. Choi, S. Hong, J. T. Abrahamson et al., "Chemically driven carbon-nanotube-guided thermopower waves," *Nature Materials*, vol. 9, no. 5, pp. 423–429, 2010.
- [14] K. Yang, M. Gu, Y. Guo, X. Pan, and G. Mu, "Effects of carbon nanotube functionalization on the mechanical and thermal properties of epoxy composites," *Carbon*, vol. 47, no. 7, pp. 1723–1737, 2009.
- [15] T. Kashiwagi, E. Grulke, J. Hilding et al., "Thermal and flammability properties of polypropylene/carbon nanotube nanocomposites," *Polymer*, vol. 45, no. 12, pp. 4227–4239, 2004.
- [16] P. Liu, K. L. White, H. Sugiyama et al., "Influence of trace amount of well-dispersed carbon nanotubes on structural development and tensile properties of polypropylene," *Macromolecules*, vol. 46, no. 2, pp. 463–473, 2013.
- [17] C. Marco, M. Naffakh, M. A. Gómez, G. Santoro, and G. Ellis, "The crystallization of polypropylene in multiwall carbon nanotube-based composites," *Polymer Composites*, vol. 32, no. 2, pp. 324–333, 2011.
- [18] M. Micusik, M. Omastova, J. Pionteck, C. Pandis, E. Logakis, and P. Pissis, "Influence of surface treatment of multiwall carbon nanotubes on the properties of polypropylene/carbon nanotubes nanocomposites," *Polymers for Advanced Technologies*, vol. 22, no. 1, pp. 38–47, 2011.
- [19] G. Z. Papageorgiou, M. Nerantzaki, I. Grigoriadou, D. G. Papageorgiou, K. Chrissafis, and D. Bikiaris, "Isotactic polypropylene/multi-walled carbon nanotube nanocomposites: the effect of modification of MWCNTs on mechanical properties and melt crystallization," *Macromolecular Chemistry and Physics*, vol. 214, no. 21, pp. 2415–2431, 2013.
- [20] M. A. L. Machado, L. Valentini, J. Biagiotti, and J. M. Kenny, "Thermal and mechanical properties of single-walled carbon nanotubes-polypropylene composites prepared by melt processing," *Carbon*, vol. 43, no. 7, pp. 1499–1505, 2005.
- [21] E. Arshid, M. Khorasani, Z. Soleimani-Javid, S. Amir, and A. Tounsi, "Porosity-dependent vibration analysis of FG microplates embedded by polymeric nanocomposite patches considering hygrothermal effect via an innovative plate theory," *Engineering with Computers*, 2021.
- [22] H. Deng, E. Bilotti, R. Zhang, and T. Peijs, "Effective reinforcement of carbon nanotubes in polypropylene matrices," *Journal of Applied Polymer Science*, vol. 118, no. 1, pp. 30–41, 2010.
- [23] M. A. Bhuiyan, R. V. Pucha, M. Karevan, and K. Kalaitzidou, "Tensile modulus of carbon nanotube/polypropylene composites—a computational study based on experimental characterization," *Computational Materials Science*, vol. 50, no. 8, pp. 2347–2353, 2011.
- [24] S. Paunekar and S. Kumar, "Effect of CNT waviness on the effective mechanical properties of long and short CNT reinforced composites," *Computational Materials Science*, vol. 95, pp. 21–28, 2014.
- [25] E. Logakis, E. Pollatos, C. Pandis et al., "Structure-property relationships in isotactic polypropylene/multi-walled carbon nanotubes nanocomposites," *Composites Science and Technology*, vol. 70, no. 2, pp. 328–335, 2010.
- [26] M. M. Zamani, A. Fereidoon, and A. Sabet, "Multi-walled carbon nanotube-filled polypropylene nanocomposites: high velocity impact response and mechanical properties," *Iranian Polymer Journal*, vol. 21, no. 12, pp. 887–894, 2012.
- [27] C. Li, H. Deng, K. Wang, Q. Zhang, F. Chen, and Q. Fu, "Strengthening and toughening of thermoplastic polyolefin elastomer using polypropylene-grafted multiwalled carbon nanotubes," *Journal of Applied Polymer Science*, vol. 121, no. 4, pp. 2104–2112, 2011.
- [28] N. G. Karsli, S. Yesil, and A. Aytac, "Effect of hybrid carbon nanotube/short glass fiber reinforcement on the properties of polypropylene composites," *Composites Part B: Engineering*, vol. 63, pp. 154–160, 2014.
- [29] D. Bikiaris, "Microstructure and properties of polypropylene/carbon nanotube nanocomposites," *Materials*, vol. 3, no. 4, pp. 2884–2946, 2010.
- [30] K. Prashantha, J. Soulestin, M. F. Lacrampe, P. Krawczak, G. Dupin, and M. Claes, "Masterbatch-based multi-walled carbon nanotube filled polypropylene nanocomposites: assessment of rheological and mechanical properties," *Composites Science and Technology*, vol. 69, no. 11–12, pp. 1756–1763, 2009.
- [31] Y. Jia, K. Peng, X.-l. Gong, and Z. Zhang, "Creep and recovery of polypropylene/carbon nanotube composites," *International Journal of Plasticity*, vol. 27, no. 8, pp. 1239–1251, 2011.
- [32] Y.-S. Shim, B.-G. Min, and S.-J. Park, "Effects of functional grafting on viscoelastic and toughness behaviors of multi-walled carbon nanotubes-reinforced polypropylene nanocomposites," *Macromolecular Research*, vol. 20, no. 5, pp. 540–543, 2012.
- [33] P. H. Wang, P. Gulgunje, S. Ghoshal, N. Verghese, and S. Kumar, "Rheological behavior of polypropylene nanocomposites with tailored polymer/multiwall carbon nanotubes interface," *Polymer Engineering & Science*, vol. 59, no. 9, pp. 1763–1777, 2019.
- [34] S. Alimirzaei, M. Mohammadimehr, and A. Tounsi, "Non-linear analysis of viscoelastic micro-composite beam with geometrical imperfection using FEM: MSGT electro-magneto-elastic bending, buckling and vibration solutions,"

- Structural Engineering and Mechanics*, vol. 71, no. 5, pp. 485–502, 2019.
- [35] A. Montazeri and R. Naghdabadi, “Study the effect of viscoelastic matrix model on the stability of CNT/polymer composites by multiscale modeling,” *Polymer Composites*, vol. 30, no. 11, pp. 1545–1551, 2009.
- [36] R. K. Duncan, R. Qiao, J. B. Bult, D. Burris, L. C. Brinson, and L. S. Schadler, “Viscoelastic behavior of nanotube-filled polycarbonate: effect of aspect ratio and interface chemistry,” *International Journal of Smart and Nano Materials*, vol. 1, no. 1, pp. 53–68, 2010.
- [37] A. Swain and T. Roy, “Viscoelastic material damping characteristics of carbon nanotubes based functionally graded composite shell structures,” *Proceedings of the Institution of Mechanical Engineers, Part L: Journal of Materials: Design and Applications*, vol. 233, no. 8, pp. 1510–1541, 2019.
- [38] H. Hirane, M. O. Belarbi, M. S. A. Houari, and A. Tounsi, “On the layerwise finite element formulation for static and free vibration analysis of functionally graded sandwich plates,” *Engineering with Computers*, 2021.
- [39] J. Huang and D. Rodrigue, “The effect of carbon nanotube orientation and content on the mechanical properties of polypropylene based composites,” *Materials & Design*, vol. 55, pp. 653–663, 2014.
- [40] J. Huang and D. Rodrigue, “Analysis of multiaxial properties of carbon nanotubes/polypropylene and nanocrystalline cellulose/polypropylene composites,” *Polymer Composites*, vol. 37, no. 4, pp. 1180–1189, 2016.
- [41] MSC, “Marc version 2010,” *Elementary Library*, vol. B, MSC Software Corporation, Newport Beach, CA, USA, 2010, <http://www.mscsoftware.com>.
- [42] L. Li, W. Li, H. Wang et al., “Investigation of Prony series model related asphalt mixture properties under different confining pressures,” *Construction and Building Materials*, vol. 166, pp. 147–157, 2018.